Neuron 49, 119–130, January 5, 2006 ©2006 Elsevier Inc. DOI 10.1016/j.neuron.2005.12.014

Enhancement of Spike-Timing Precision by Autaptic Transmission in Neocortical Inhibitory Interneurons

Alberto Bacci[1] and John R. Huguenard[1,*]
[1] Department of Neurology and Neurological Sciences
Stanford University School of Medicine
Stanford, California 94305

Summary

In vivo studies suggest that precise firing of neurons is important for correct sensory representation. Principal neocortical neurons fire imprecisely when repeatedly activated by fixed sensory stimuli or current depolarizations. Here we show that in contrast to pyramidal neurons, firing in neocortical GABAergic fast-spiking (FS) interneurons is quite precise. FS interneurons are self-innervated by powerful GABAergic autaptic connections reliably activated after each spike, suggesting that autapses strongly regulate FS-cell spike timing. Indeed, blockade of autaptic transmission degraded temporal precision in multiple ways. Under these conditions, realistic dynamic-clamp hyperpolarizing autapses restored precision of spike timing, even in the presence of synaptic noise. Furthermore, firing precision was increased in pyramidal neurons by artificial GABAergic autaptic conductances, suggesting that tightly coupled synaptic feedback inhibition regulates spike timing in principal cells. Thus, well-timed inhibition, whether autaptic or synaptic, facilitates precise spike timing and promotes synchronized cortical network oscillations relevant to several behaviors.

Introduction

The neocortex is the final destination of sensory information and is the site where this information is processed and eventually integrated into several behavioral and cognitive functions. Cortical neurons process and transmit information by integrating their synaptic inputs and generating discrete trains of action potentials (APs) that can be precisely timed. Consistent spike trains in response to repetitive identical stimuli may be important in building a neuronal code based on spike timing (Mainen and Sejnowski, 1995; Stevens and Zador, 1995; Grothe and Klump, 2000; VanRullen et al., 2005). In vivo studies suggest that principal neocortical neurons fire in response to identical sensory stimuli with a large trial-to-trial variability (Shadlen and Newsome, 1998; Carandini, 2004). Yet, neurons in other CNS areas such as thalamus and retina fire faithfully in response to repeated presentations of the same sensory stimulus (Reich et al., 1997; Kara et al., 2000; Reinagel and Reid, 2002). Moreover, neurons encode aspects of the fine temporal structure of sensory stimuli in visual cortices (Gur et al., 1997; Buracas et al., 1998) and invertebrate preparations (de Ruyter Van Steveninck et al., 1997).

*Correspondence: john.huguenard@stanford.edu

In neocortical slices in vitro, identical step current injection stimulations produce very jittery firing in pyramidal neurons, but spike-timing precision is significantly improved when stimuli contain synaptic-like noise, mimicking the continuous synaptic bombardment that pyramidal neurons receive during dynamic sensory inputs (Mainen and Sejnowski, 1995).

Cortical structures such as hippocampus and neocortex undergo network oscillations in the theta and gamma frequency range during dynamic cognitive tasks and varying sensory stimulations, and it has been proposed that this oscillatory activity might be important in binding sensory information (McBain and Fisahn, 2001; Buzsaki and Draguhn, 2004). Cortical oscillations are believed to be generated and maintained by GABAergic interneurons, which synchronize the firing of large groups of pyramidal neurons (McBain and Fisahn, 2001; Fricker and Miles, 2001; Freund, 2003). In particular, due to the specific innervation pattern on pyramidal cell bodies (Thomson et al., 1996; Tamas et al., 1997a; Kawaguchi and Kubota, 1998; Xiang et al., 2002), it is believed that a specific subtype of interneuron—the parvalbumin-positive, fast-spiking (FS) basket cell—controls the synchronized output of cortical principal cells (Freund, 2003). Basket cells fire synchronously during cortical oscillations (Tamas et al., 2000), by virtue of their highly interconnected network formed by both electrical and GABAergic chemical synapses (Tamas et al., 1998; Galarreta and Hestrin, 1999; Gibson et al., 1999; Beierlein et al., 2000). In particular, basket cells in the hippocampus are known to fire very precisely during theta and gamma oscillations (Penttonen et al., 1998; Klausberger et al., 2003; Hajos et al., 2004; Somogyi and Klausberger, 2005), suggesting that they might possess intrinsic mechanisms that promote their spike timing and thus precision.

We recently demonstrated that FS neocortical interneurons innervate themselves, generating robust GABAergic autaptic transmission (Bacci et al., 2003a). Autaptic transmission is selective for FS basket cells (Tamas et al., 1997b; Bacci et al., 2003a) and results in a fast and reliable shunting inhibition, which is activated every time a FS cell fires an action potential (Bacci et al., 2003a). The tight temporal link between a spike and a closely following large GABAergic conductance makes autaptic transmission a very good candidate in controlling the timing of subsequent APs and thus eventually in modulating spike timing during a train.

To address the role of autaptic transmission in regulating the precision of spike timing, we recorded from FS interneurons in acute brain slices of juvenile rats in the presence of ionotropic glutamate receptor blockers. This simplified preparation, in which autaptic transmission is kept intact but excitatory neurotransmission is abolished, provided a convenient means to examine the functional properties of autapses.

We found that FS interneurons are characterized by highly precise AP timing, as compared to large pyramidal cells, and that GABAergic autaptic transmission plays a major role in improving the precision of spike

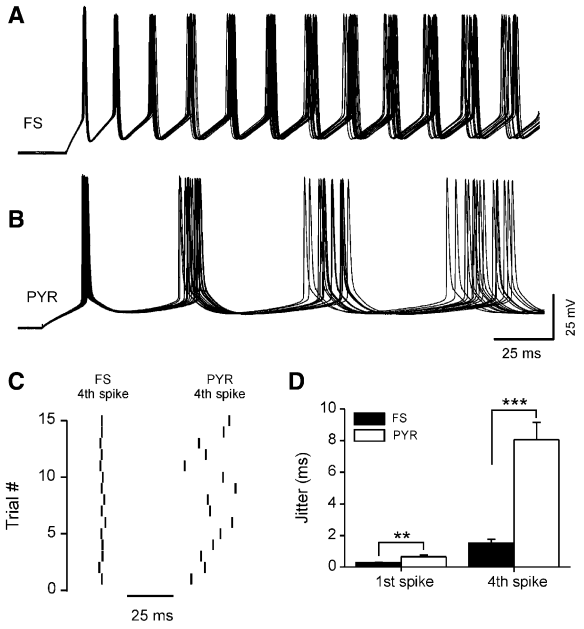

Figure 1. Neocortical FS Interneurons Fire More Precisely than Pyramidal Neurons

(A) Overlapped responses to 15 identical suprathreshold DC current injections (200 pA) in a FS interneuron. Resting membrane potential (RMP) = −66 mV.

(B) Overlapped responses to 15 identical suprathreshold DC current injections (250 pA) in a pyramidal neuron. RMP = −61 mV. Note progressive increase in jitter during the train in both FS and pyramidal cell (A and B).

(C) Raster plot of the fourth spikes of the cells of (A) and (B). Each vertical line indicates an action potential.

(D) Mean jitter of the first and fourth spikes in FS cells (black columns) and in pyramidal neurons (white columns). **p < 0.01; ***p < 0.001, n = 14 and 10 FS and pyramidal cells, respectively.

times in FS cells. This was true also when elevated and variable spontaneous synaptic activity was included in the stimulation waveform. Moreover, we found that GABAergic feedback inhibition could act in a similar manner to autaptic transmission to enhance spiking precision in pyramidal neurons.

Results

FS Interneurons Fire More Precisely than Pyramidal Neurons

Whole-cell current-clamp experiments were obtained in rat neocortical slices. Neurons were visualized by infrared videomicroscopy, and FS interneurons were identified as round multipolar cells without an apical dendrite. Current-clamp characterization showed typical high-frequency firing (frequency range: 40–86 Hz, n = 14) in response to depolarizing current steps (Kawaguchi and Kubota, 1997; Beierlein et al., 2003; Bacci et al., 2003a, 2003b). Pyramidal neurons were identified by their typical large soma size and the presence of a thick apical dendrite oriented toward the pial surface. Pyramidal neurons were characterized by lower firing frequency (range: 5–18 Hz, n = 12) and much broader action potential than FS interneurons.

Under conditions of excitatory neurotransmission blockade, FS and pyramidal neurons were depolarized multiple times by identical near-threshold DC current injections, which yielded action potential trains in the frequency ranges mentioned above. Each cell type showed a nearly constant rate of firing during repeated trains (CV = 0.03 ± 0.003 versus 0.04 ± 0.004 FS versus pyramidal cells, n = 14 and 12, respectively; $p > 0.05$, independent t test). However, FS and pyramidal neurons showed a large difference in spike-timing precision across different stimulation trials. We quantified spike-timing precision as spike jitter, defined as the standard deviation of the ordinal spike times across multiple identical stimulation trials. Jitter increased progressively during the train in both FS and pyramidal neurons, yet FS cells showed a very high degree of precision compared to pyramidal neurons (Figures 1A–1C). For example, spike jitter was significantly higher in pyramidal neurons than FS cells at the first and fourth spike in the train (first spike jitter: 0.27 ± 0.03 versus 0.65 ± 0.11 ms, n = 14 and 10 FS and pyramidal cells, respectively; $p < 0.01$, independent t test; fourth spike jitter: 1.5 ± 0.2 versus 8.1 ± 1.1 ms, n = 14 and 10 FS and pyramidal cells, respectively; $p < 0.001$, independent t test; Figure 1D). As discussed below, the precision of spike timing increases with frequency, and thus the higher precision of FS cells may result from their faster output rate. To test this possibility, we examined spike timing in pyramidal neurons by using strong intracellular current injections that produced maximal firing without inducing spike inactivation. Under these conditions, pyramidal neurons could fire sustained action potentials at frequencies up to 33 Hz (mean: 30.6 ± 0.8 Hz, n = 5), yet the spike jitter (fourth spike: 2.5 ± 0.4 ms) remained higher than obtained with near-threshold firing (~40 Hz) of FS neurons ($p < 0.02$, independent t test).

Autaptic Transmission in FS Interneurons Is Robust but Transient

To test the role of autaptic transmission in regulating spike timing in FS interneurons, we developed a dynamic-clamp experiment aimed at generating realistic artificial autaptic conductances, after blocking natural autaptic transmission pharmacologically. Several physiological properties of autapses have been reported, including latency, decay time, and magnitude (Bacci et al., 2003a). However, their short-term dynamics are not yet known. Hence, we characterized short-term plasticity during repetitive activation of autapses in FS interneurons. For these experiments, we used a high-chloride-containing intracellular solution to maximize detection of autaptic signals. We generated trains of brief depolarizations (0.4–1.0 ms to 0 mV from V_h = −70 mV), each triggering an AP and an autaptic response, at different frequencies (10, 30, 50, 60, and 100 Hz) and measured the time-dependent depression of the autaptic inhibitory synaptic currents (autIPSCs) during the train (Figures 2A and 2B). Chloride accumulation during autaptic train was ruled out as a contributing factor to autaptic depression because voltage-clamp experiments revealed that the time course of use-dependent depression for both autaptic and synaptic inhibition was unaffected by changes in holding potential that would have influenced the degree of intracellular Cl^- load (data not shown, cf. Huguenard and Alger, 1986). autIPSCs were found to undergo moderate depression even at

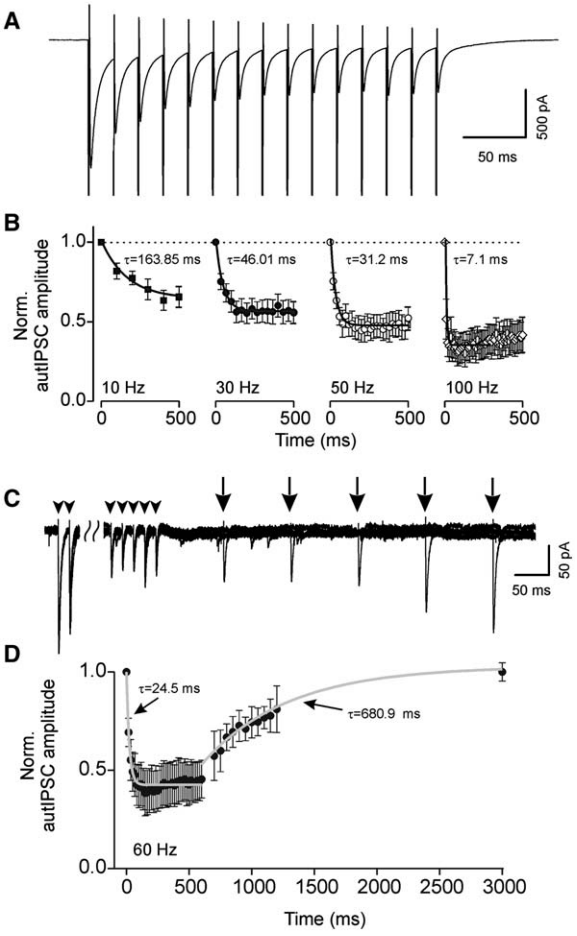

Figure 2. Depression and Recovery of Autaptic Transmission in FS Interneurons

(A) Representative trace of autaptic depression, during 50 Hz stimulation in a FS cell. Stimuli consisted of 0.5 ms voltage depolarization to 0 mV from a holding potential of −70 mV. Shown is the average of 20 traces. The sodium currents elicited by the depolarizations have been truncated for display purposes.

(B) Plot of mean autaptic depression at different stimulation frequencies. Responses were normalized to first autIPSCs. The black lines superimposed on the symbols are mono-exponential decays. τ = decay time constant (n = 8 cells).

(C) Representative traces of autaptic recovery after depression induced by 600 ms long trains at 60 Hz. Overlapped traces with autaptic stimulations elicited following the train after 100–500 ms in 100 ms increasing steps. For display purposes, the first two and last five responses in the 60 Hz autaptic trains are shown. Arrowheads indicate autaptic stimulations within the trains, and arrows point to autaptic stimulations following the trains. Autaptic stimulus artifacts have been digitally canceled. Autaptic transmission evoked as indicated in (A).

(D) Plot of mean autaptic recovery after depression caused by 600 ms long trains at 60 Hz. Responses were normalized to first autIPSCs. Gray lines are mono-exponential fits and shown are decay and recovery time constant (τ) values.

frequencies as low as 10 Hz. This, together with their low failure rate (Bacci et al., 2003a), indicates that FS cell autapses release GABA with high release probability. For each given frequency, normalized autIPSC peak amplitudes during a train were averaged across cells (n = 8). The resulting curves were fitted with exponential functions having decay time constants of 164, 46, 31, 25, and 7 ms at 10, 30, 50, 60, and 100 Hz, respectively (Figures 2B and 2D). Further, we determined that autIPSC recovery rate was 681 ms (n = 8; Figures 2C and 2D). Based on the known properties of autapses, including those of autIPSC short-term plasticity outlined above, we implemented dynamic-clamp autapses, which were triggered by actual action potentials evoked in recorded neurons.

Dynamic-clamp autapses were then introduced in separate current-clamp experiments obtained with physiological level of $[Cl]_i$. For these experiments, the artificial autaptic conductance had properties essentially the same as those recorded in voltage-clamp mode, i.e., an average peak conductance of 6 nS, a delay of 1 ms, and a decay time constant of 6.8 ms (see Figure S2A in the Supplemental Data available online; Bacci et al., 2003a). A use-dependent decay of the artificial autaptic conductance was present (Figures S2B and S2C), with similar properties of those reported in Figure 2 and based on the approach of Fuhrmann et al. (2002b).

Autaptic Transmission Enhances Spike-Timing Precision in FS Interneurons

We then tested whether autaptic transmission in FS interneurons was important in setting the spike timing during action potential trains. In current-clamp, FS interneurons received ten identical suprathreshold current injections while maintaining constant V_{rest}. In control conditions, FS interneurons generated highly faithful firing in response to identical DC stimulation. Indeed, action potentials occurred with little jitter across identical trials (Figure 3A). When autapses (and other inhibitory synapses) were blocked by the $GABA_A$ receptor antagonist gabazine (10 μM), the same DC stimuli generated less precise firing, as indicated by highly jittery responses (Figure 3B). Then, in the continued presence of gabazine, dynamic-clamp autaptic transmission was specifically introduced as in Figure S2. Realistic artificial autaptic transmission restored precision of spike timing (Figure 3C), which was subsequently lost when the dynamic clamp was switched off (Figure 3D). As indicated earlier, spike jitter across different trials increased linearly during the train. Jitter slope (measured as jitter/time) over the first 10 to 15 spike latencies was then computed. Gabazine application increased jitter slope, an effect that was reversed by addition of dynamic-clamp autaptic transmission (Figure 3E). The gabazine-dependent effect on spike jitter was most prominent when neurons fired between 40 and 80 Hz, which is in the gamma-frequency range. Autaptic transmission did not show any notable effect on spike-timing precision at higher frequencies (>100 Hz; Figure S1). On average, jitter slope was 0.019 ± 0.001 versus 0.03 ± 0.004 control versus gabazine. Dynamic-clamp autaptic transmission reversibly decreased mean jitter slope to 0.015 ± 0.002 (Figure 3F; n = 14, RM-ANOVA with post hoc comparisons: $p < 0.02$ control versus gabazine; $p < 0.001$ gabazine versus dynamic-clamp autIPSCs; $p < 0.001$ dynamic-clamp autIPSCs ON versus dynamic-clamp autIPSCs OFF; $p > 0.1$ control versus dynamic-clamp autIPSCs ON and flat DC gabazine versus dynamic-clamp autIPSCs OFF).

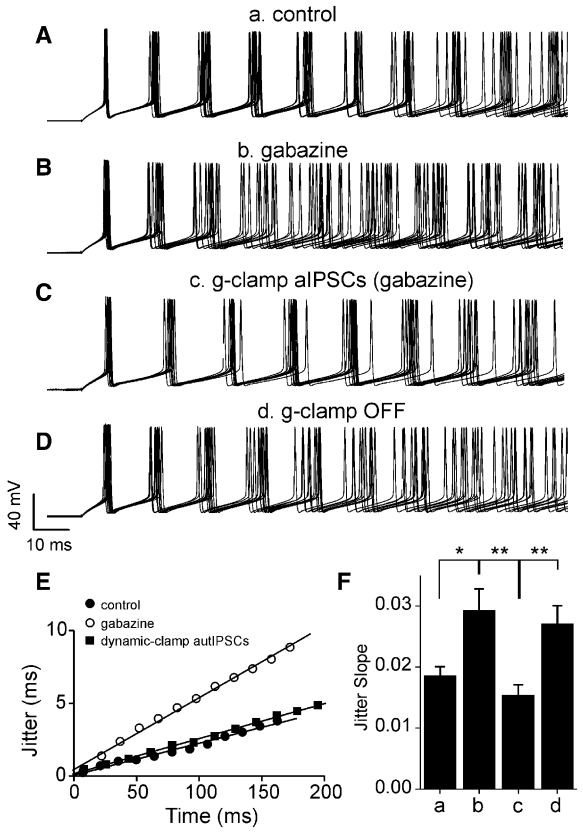

Figure 3. Autaptic Transmission Modulates Spike-Timing Precision in FS Interneurons

(A–D) Overlapped traces of a FS interneuron firing induced by ten identical DC depolarizations in control conditions (A), in the presence of 10 μM gabazine (B), with gabazine but with dynamic-clamp autapses (C), and a subsequent set of flat DC depolarizations in the presence of gabazine and with dynamic-clamp autaptic transmission switched off. DC depolarization amplitude: 300 pA.

(E) Plot of jitter versus time for the experiment shown in (A)–(C). Data were well fitted by linear relationships (black lines).

(F) Plot of mean jitter slope computed from linear fits such as those shown in (E). a, control; b, in the presence of gabazine; c, in the presence of gabazine with dynamic-clamp autapses on; d, dynamic autapses off (in the continued presence of gabazine).

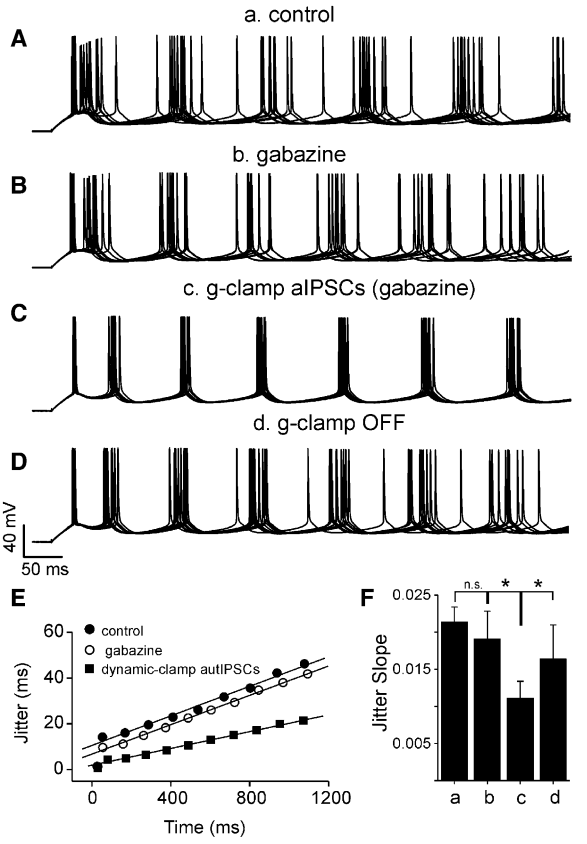

Figure 4. Artificial GABAergic Autaptic Transmission Enhances Spike-Timing Precision in Pyramidal Neurons

(A–D) Overlapped traces of a pyramidal neuron firing induced by ten identical DC depolarizations in control conditions (A), in the presence of 10 μM gabazine (B), with gabazine but with dynamic-clamp autapses (C), and a subsequent set of in the presence of gabazine and with dynamic-clamp autaptic transmission switched off (D). DC depolarization amplitude: 350 pA.

(E) Plot of jitter versus time for the experiment shown in (A)–(C). Data were well fitted by linear relationships (black lines).

(F) Plot of mean jitter slope computed from linear fits such as those shown in (E). a, control; b, in the presence of gabazine; c, in the presence of gabazine with dynamic clamp autapses on; d, dynamic-clamp autapses off (in the continued presence of gabazine).

Artificial Autapses Modulate Spike-Timing Precision in Neocortical Pyramidal Neurons

To test whether precisely timed feedback inhibition could play a general role in modulating spike timing, we recorded from large layer V pyramidal neurons and introduced artificial GABAergic autaptic transmission in this cell type, which normally does not possess GABAergic autapses and shows a low spike-timing precision. When exposed to identical DC current injections, pyramidal neurons responded with highly jittery responses, which were not affected by gabazine (Figures 4A and 4B), indicating that ongoing spontaneous GABAergic synaptic transmission plays a small role in pyramidal cell precision firing during repeated trains. When artificial GABAergic autapses were introduced via dynamic clamp, precision in pyramidal neurons markedly increased (Figure 4C), as had occurred in FS cells. Mean jitter slope was 0.02 ± 0.002 in control, 0.019 ± 0.004 in gabazine, 0.01 ± 0.002 with dynamic-clamp autIPSCs, and 0.016 ± 0.005 when dynamic clamp was switched off (Figure 4F, n = 6; RM-ANOVA, with post hoc comparisons: $p > 0.4$ control versus gabazine; $p < 0.02$ gabazine versus dynamic-clamp autIPSCs; $p < 0.03$ dynamic-clamp autIPSCs ON versus dynamic-clamp autIPSCs OFF).

Autaptic Transmission Determines the Amount of Spike-Frequency Adaptation in FS Interneurons

Autaptic transmission in FS interneurons is a very robust and reliable source of feedback inhibition. Yet, during sustained firing it tends to dissipate (cf. Figure 2), likely due to use-dependent reduction in release probability. We have previously shown that autaptic transmission influences changes in firing rates during sustained stimuli (Bacci et al., 2003a). Here, we directly tested whether

short-term dynamics of autaptic transmission during a train could affect spike frequency of FS interneurons. In control conditions, when spike trains were evoked by suprathreshold DC current injection, FS interneurons showed little or no spike-frequency adaptation, measured as the difference of instantaneous frequency between the first and the tenth spike interval in the train. When autaptic transmission was blocked by gabazine, firing frequency increased, especially in the first part of the train, in agreement with our previously published observation from perforated-patch experiments (Bacci et al., 2003a). Spike-frequency adaptation increased in the presence of gabazine (mean difference between first and tenth instantaneous frequency, $\Delta f = 7.4 \pm 2.5$ versus 14.4 ± 4.1 Hz, control versus gabazine; $p < 0.01$; RM-ANOVA with post hoc comparisons; $n = 11$; Figures 5A and 5B), but when dynamic-clamp autaptic transmission was introduced, adaptation was dramatically reduced ($\Delta f = 1.04 \pm 1.8$ Hz; $p < 0.001$; Figures 5A and 5B). Increasing dynamic-clamp autaptic strength to 10 nS resulted in a switch from adapting to accelerating firing behavior ($\Delta f = -4.6 \pm 1.3$ Hz; Figure 5C). To test whether short-term plasticity of autapses (e.g., Figure 2) was responsible for the anti-accomodating effect, we removed use-dependent depression of dynamic-clamp autIPSCs, which largely eliminated the effect on spike-frequency adaptation ($\Delta f = 5.1 \pm 2.7$; Figure 5C). Finally, when dynamic clamp was switched off, FS interneurons again showed prominent adapting firing behavior ($\Delta f = 14.7 \pm 4.7$ Hz; Figures 5A–5C). These data indicate that autaptic transmission strongly modulates spike-frequency adaptation in FS interneurons.

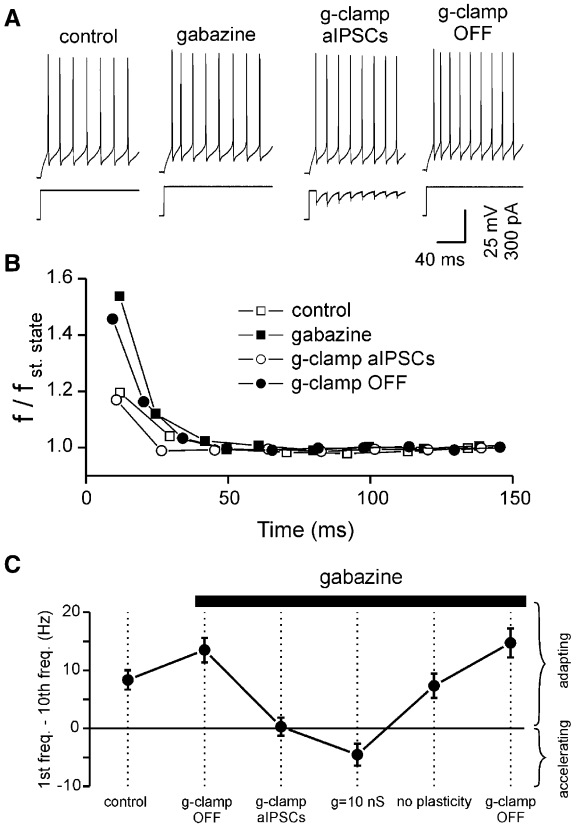

Figure 5. Spike-Frequency Adaptation Is Modulated by Autaptic Transmission in FS Interneurons

(A) Representative traces relative to a FS cell firing in response of single depolarizing DC current injection in control and in the presence of gabazine both with and without dynamic-clamp autaptic transmission.

(B) Plot of instantaneous frequency versus time in the cell of (A) with the same experimental manipulations. Frequency was normalized to the steady-state frequency calculated after the tenth spike interval.

(C) Mean spike frequency adaptation measured as the instantaneous frequency of the tenth subtracted from the first spike interval. The black bar indicates the presence of gabazine ($n = 31$). Note that when autaptic conductance was increased to 10 nS, firing behavior became accelerating. Removal of short-term plasticity resulted in a decreased effect of autaptic conductances on spike-frequency adaptation.

Autaptic Modulation of Regularity of Firing in FS Interneurons

In addition to the effects on spike-frequency adaptation, autaptic transmission might modulate the regularity of steady-state firing and thus contribute to precise FS spike timing. To test this hypothesis, we analyzed spike regularity in FS interneurons in control, in the presence of gabazine, and with computer-generated autaptic responses. In control conditions, steady-state action potential firing was regular, as spikes occurred precisely and did not substantially deviate from the regular spike-timing pattern calculated from their averaged steady-state frequency (vertical bars in Figure 6A). When autaptic transmission was blocked by gabazine, interspike intervals became more irregular, as action potentials often deviated from the theoretical regular spike timing calculated from their average steady-state frequency (Figures 6B and 6D). Dynamic-clamp autaptic conductance restored action potential regularity (Figure 6C). This autaptic-mediated effect on spike regularity was also evident as highly variable frequency-time plots in the presence of gabazine, in contrast to control and dynamic-clamp autIPSCs (Figure 6E). We quantified firing regularity within each action potential train by using a modified coefficient of variation of interspike intervals (CV2, see Experimental Procedures; Holt et al., 1996). Compared to standard coefficient of variation (CV), CV2 is less sensitive to spike-rate variations such as those that occur during accommodating spike trains (Figure 5) and thus represents a more accurate estimate of the regularity of neuronal firing if the mean rate changes over time (Holt et al., 1996). Higher values of CV2 indicate decreased spike regularity. We found that CV2 increased in the presence of gabazine (mean CV2: 0.04 ± 0.004 versus 0.05 ± 0.006, control versus gabazine; $p < 0.05$, RM-ANOVA with post hoc comparisons, $n = 7$) and that computer-generated autaptic transmission reversibly reduced CV2 (dynamic-clamp on: 0.03 ± 0.003, dynamic clamp off: 0.05 ± 0.06, $p < 0.01$).

CV2 analysis performed on pyramidal neurons revealed that this cell type also fires more regularly in the presence of artificial GABAergic autaptic transmission (mean CV2: 0.045 ± 0.006 versus 0.033 ± 0.003 control versus dynamic clamp; $p < 0.01$ RM-ANOVA with post hoc comparisons, $n = 6$). As with jitter, gabazine alone did not produce a change in discharge regularity of pyramidal neuron firing (mean CV2 in gabazine: 0.046 ± 0.005, $p > 0.3$).

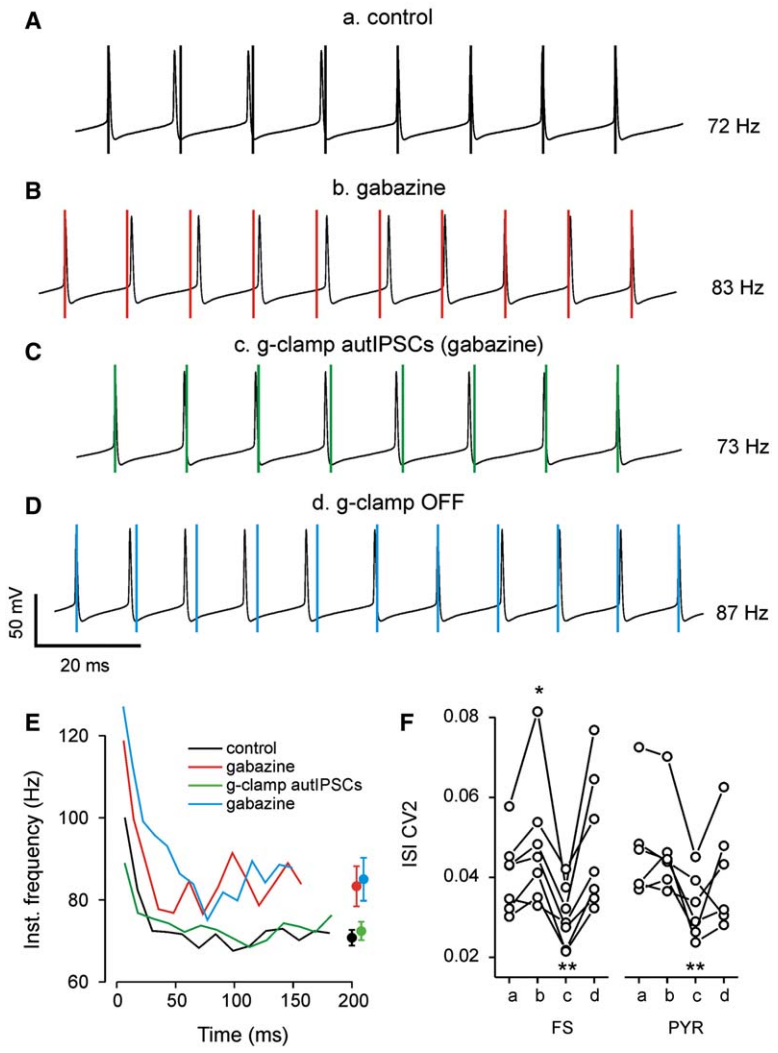

Figure 6. Autaptic Modulation of Spike Regularity

(A–D) Representative traces of single action potential trains elicited in a FS interneuron by depolarizing current injections in control conditions (A), in the presence of gabazine (B), in the presence of gabazine but with dynamic-clamp autIPSCs (C), and a subsequent DC depolarization in the presence of gabazine and with dynamic-clamp autaptic transmission switched off (D). DC injections = 325 pA in all cases. Vertical lines mark regular inter-spike intervals at the steady-state frequencies calculated after the third spike and indicated next to each case. The first three spikes in each train have been omitted for display purposes.

(E) Plot of instantaneous firing frequency versus time for the cell of (A)–(D). Color code as in (A)–(D): black, control; red, gabazine; green, dynamic-clamp autIPSC; blue, dynamic clamp off. Note the more jagged lines in gabazine as compared to conditions in which autaptic transmission was present in control and when autapses were artificially introduced with dynamic clamp. Filled symbols represent the mean instantaneous frequency calculated after the fourth spike intervals. Error bars are standard deviation (SD). Color codes as in (A)–(D). Note larger SD in the absence of either natural or dynamic-clamp autapses.

(F) Plot of interspike interval CV2 in FS cells (left) and pyramidal neurons (right). a, control; b, in the presence of gabazine; c, in the presence of gabazine with dynamic-clamp autapses on; d, subsequent depolarization with dynamic-clamp autapses off (in the presence of gabazine). CV2 was calculated in FS interneurons and pyramidal cells in each sweep and averaged across 10 to 20 sweeps each for each condition. Note the lack of effect of gabazine in pyramidal neurons and how dynamic-clamp autaptic transmission changes spike regularity in this cell type. *$p < 0.05$; **$p < 0.01$. In all but one FS cell, CV2 was increased by gabazine, while no consistent effect was seen in pyramidal neurons.

Role of Autaptic Hyperpolarization versus Conductance in Regulating Spike-Timing Precision in FS Interneurons

We have previously shown that GABAergic autaptic transmission results in shunting inhibition when single spikes are triggered by brief depolarizations from resting membrane potential (Bacci et al., 2003a). However, during sustained repetitive firing, the membrane potential is on average more depolarized, increasing the driving force for $GABA_A$ receptor-mediated events. Thus, activation of autapses during a spike train results in a series of hyperpolarizing currents which dissipate over time (Figures S2B and S2C). In the presence of gabazine to block natural autapses, we used dynamic clamp to test whether autapses modulate spike-timing precision through a voltage or a conductance effect. We injected either action potential-triggered current-based IPSCs or a constant GABAergic conductance. Hyperpolarizing current-based autaptic IPSCs were found to reduce both spike jitter and CV2 compared to DC current injection (Figure 7B versus Figure 8A), thus improving precision of spike timing (Figure 7B). By contrast, precision was decreased significantly by a constant GABAergic conductance (Figure 7C). On average, jitter slope was 0.025 ± 0.0045 with simple DC versus 0.020 ± 0.003 with hyperpolarizing currents ($p < 0.005$ DC versus current-based IPSPs; n = 5). Constant GABAergic conductance increased jitter slope to 0.043 ± 0.01 ($p < 0.05$, both for DC versus constant conductance and current-based IPSPs versus constant conductance comparisons; n = 5), which returned to 0.023 ± 0.007 when dynamic-clamp autaptic events were disabled ($p > 0.8$, DC series 1 versus 2 comparison; n = 5). CV2 showed a similar trend (CV2 = 0.045 ± 0.005 versus 0.037 ± 0.004 $p < 0.005$ DC versus current-based autaptic IPSPs; 0.044 ± 0.008 versus 0.06 ± 0.009, $p < 0.02$, DC versus constant conductance). These data indicate that the autaptic effect on FS cell spike timing is due to the hyperpolarizing component of GABAergic autaptic transmission rather than to its shunting mechanism. Moreover,

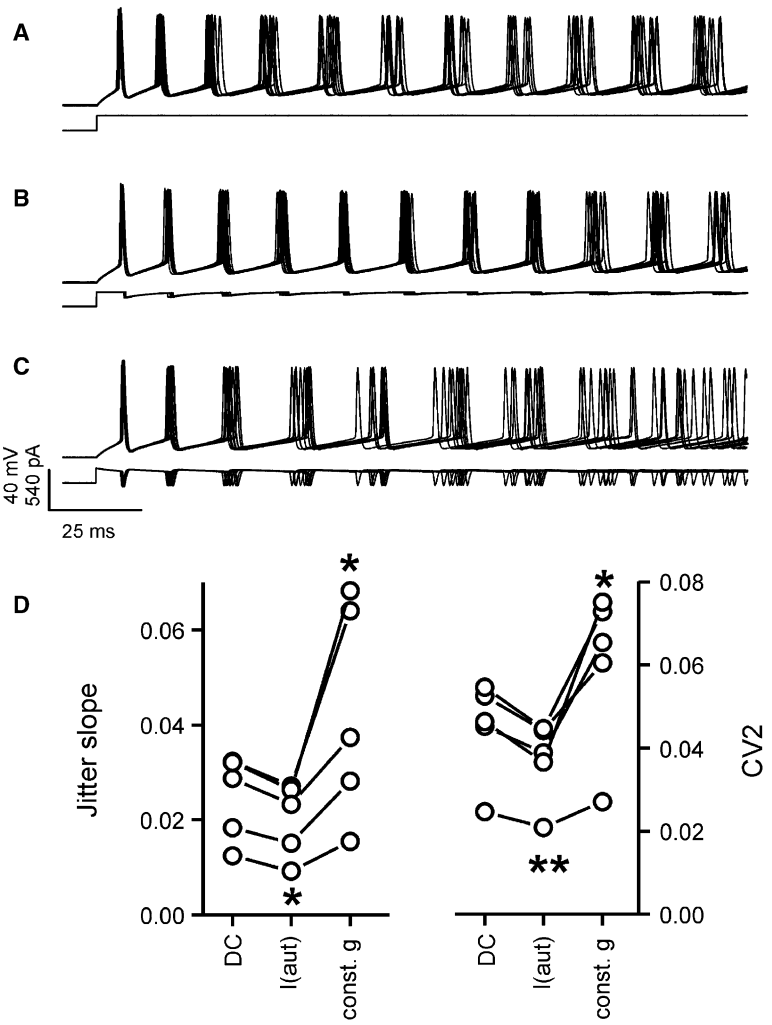

Figure 7. Autaptic Transmission Increases Spike-Timing Precision through Inter-Spike Hyperpolarizations

(A–C) Overlapped traces of a FS cell firing induced by ten identical DC depolarizations in control conditions (A) and with current-based autaptic IPSPs (B) or with a tonic GABAergic conductance (C) introduced by dynamic clamp. All traces are in the presence of gabazine (10 μM) and DL-APV and DNQX (100 and 20 μM, respectively). Note that firing precision is increased by hyperpolarizing autaptic currents but not by a constant GABAergic conductance.

(D) Summary plot of jitter slope (left) and CV2 (right). I(aut), autaptic hyperpolarizing current; const. g, tonic GABAergic conductance. *p < 0.05; **p < 0.01, paired t test, compared to DC.

these results suggest that in FS cells a tonic GABAergic conductance can negatively influence precision of spike timing, thus decreasing faithful firing.

Role of Synaptic Noise in Spike-Timing Precision in FS Interneurons

Neocortical FS interneurons are impinged upon by a myriad of synaptic contacts, both glutamatergic and GABAergic. Indeed, synaptic activity is known to influence spike timing in several brain areas, including the neocortex (Mainen and Sejnowski, 1995; Hasenstaub et al., 2005), thalamus (Blitz and Regehr, 2003, 2005), and cerebellum (Carter and Regehr, 2002). We tested whether autapses would influence spike-timing precision under conditions of dynamic-clamp spontaneous synaptic activities in the presence of ionotropic synaptic blockers (APV, DNQX, and gabazine). We generated four protocols of spontaneous synaptic activity with varying amplitudes and/or frequencies (see Experimental Procedures). The first protocol was designed to mimic sEPSCs and sIPSCs as typically recorded in our cortical slice preparation (frequency = 20 and 5 Hz for sEPSCs and sIPSCs, respectively, with a mean peak conductances of 0.25 ± 0.25 and 0.75 ± 0.75 nS, respectively see Figure S3 for sEPSCs and Bacci et al., 2003b, for sIPSCs). We increased noise in other protocols by linearly scaling frequency and/or amplitude of both sEPSCs and sIPSCs.

In all of our studies of spike-timing precision and regularity, it was critical to define a fixed reference point from which precision was calculated, i.e., the onset of the DC current depolarization. To better simulate stochastic spontaneous synaptic activity unlinked to the DC step, we presented FS interneurons with ten shuffled trials for each synaptic protocol. Within each block of ten trials sPSCs were re-randomized (Figure S4D), resulting in sweeps with different spontaneous synaptic events. The precision of spike timing decreased as sPSC amplitude and/or frequency was increased (Figure 8C, Table S1). Dynamic-clamp autapses reduced spike jitter and CV2 under all noise conditions (see example traces in Figures 8A and 8B, Table S1) indicating that autaptic transmission robustly improves spike-timing precision and regularity even in the presence of high synaptic noise.

Discussion

In the nervous system, information is encoded by the generation of sequences of all-or-none identical action

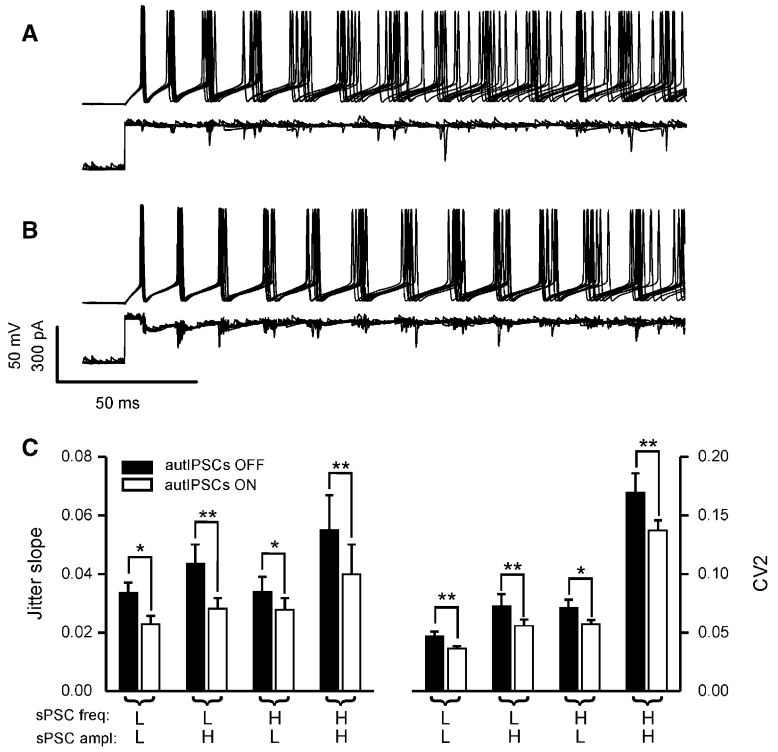

Figure 8. Autaptic Modulation of Spike-Timing Precision in the Presence of Ongoing Spontaneous Synaptic Activity

(A–B) Overlapped traces showing FS interneuron firing induced by ten identical DC depolarizations in control conditions (A) and with computer-generated autaptic conductances (B). All traces are in the presence of dynamic-clamp spontaneous synaptic activity (both sEPSCs and sIPSCs) and with gabazine (10 μM), DL-APV, and DNQX (100 and 20 μM, respectively) in the extracellular medium. These example traces refer to protocol 3 (see Experimental Procedures), i.e., high frequency and low amplitude sPSCs, with voltage responses in upper traces, and current injections below. Note the improvement in spike-timing precision produced by autaptic transmission, even in the presence of high-frequency synaptic noise.

(C) Summary plot of jitter slope (left) and CV2 (right) in the absence (autIPSCs OFF, black columns) and in the presence (autIPSCs ON, white bars) of dynamic-clamp autapses with ongoing dynamic-clamp synaptic sEPSCs and sIPSCs. sPSC freq L (low): 20 and 5 Hz, sEPSCs and sIPSCs, respectively. sPSC freq. H (high): 200 and 50 Hz sEPSCs and sIPSCs, respectively. sPSC ampl. L (low): sEPSCs, 0.25 nS mean amplitude; sIPSCs, 0.5 nS mean amplitude. sPSC ampl. H (high): sEPSCs, 0.75 nS mean amplitude; sIPSCs, 1.5 nS mean amplitude *$p < 0.05$; **$p < 0.01$, paired t test.

potentials. The details of the temporal pattern of such spike activity would be irrelevant if the neuronal code was based on mean firing rates. In contrast, patterns of precisely timed action potentials in responses to identical stimulations suggest that neurons might actually rely on a code based on spike timing, which can be used to carry information (Mainen and Sejnowski, 1995; de Ruyter Van Steveninck et al., 1997; Grothe and Klump, 2000). This issue is still matter of debate, and it is likely that these two different views on the neuronal code might be appropriate in different contexts of sensory representation and information processing (Fairhall et al., 2001).

Here, we show that neocortical layer V FS interneurons fire very precisely when exposed to the same identical near-threshold DC current depolarizations, even in the presence of synaptic noise, in contrast to pyramidal neurons, which responded to similar stimuli with very jittery responses. This result could be at least partially due to differences in the firing rate of the two cell types, as spike-timing precision increases as a function of frequency in both cell types. Our analysis focused on sustained firing frequencies that are typical for both cell types reported in vivo during persistent activity (e.g., Hasenstaub et al., 2005). The imprecise firing of pyramidal neurons is in agreement with previously published in vitro data (Mainen and Sejnowski, 1995) and is also consistent with responses obtained in vivo from principal neurons in response to identical sensory stimuli (Shadlen and Newsome, 1998; Carandini, 2004).

The large difference in spike-timing precision between FS and pyramidal neurons might be due to differential expression of specific ion channels (Schreiber et al., 2004), which might increase membrane potential noise between spikes in pyramidal cells and promote trial-to-trial variability of spike-timing precision (Carandini, 2004). On the other hand, the absence of synaptic-like noise in brain slices has been suggested to be a source of spike jitter (Mainen and Sejnowski, 1995), suggesting that constant synaptic bombardment on pyramidal neurons plays a role in spike-timing modulation.

One possible mechanism regulating the high spike-timing precision in FS interneurons might be the robust and reliable GABAergic autaptic transmission that is specific to this interneuronal subtype (Bacci et al., 2003a). After each spike, a large autaptic response is generated, which transiently decreases the likelihood of another spike (Bacci et al., 2003a) and can thus be instrumental in regulating the timing or occurrence of action potentials during a train. Indeed, in FS interneurons, pharmacological blockade of GABAergic autaptic transmission dramatically degraded precision of spike timing. Gabazine will block both autaptic transmission and ongoing spontaneous synaptic inhibition, a prominent feature in FS cells (Bacci et al., 2003b). Moreover, gabazine might block a tonic GABAergic membrane conductance (Stell and Mody, 2002; Semyanov et al., 2004; Farrant and Nusser, 2005) and might therefore influence spike timing in FS interneurons independently of GABAergic autapses. Under our experimental conditions, tonic and mean spontaneous inhibition contribute to <3% of total membrane conductance (Bacci et al., 2003a). Furthermore, when gabazine was applied to pyramidal neurons, no change in spike jitter was detected.

All together, these results suggest that ongoing synaptic GABAergic inhibition (i.e., non-autaptic) plays a small role in shaping the firing patterns of cortical neurons in vitro.

To confirm the role of autaptic transmission on spike-timing precision in FS interneurons, we simulated spike-triggered autaptic conductances using dynamic clamp, in the presence of gabazine. Dynamic-clamp conductances injected in FS cell bodies through the patch pipette will resemble real autaptic transmission, as suggested by the anatomical localization of autapses mostly around the soma and the proximally dendrites in FS interneurons (Tamas et al., 1997b). Computer-generated autapses were designed to closely approximate the properties of FS autapses, including those of short-term depression, reflecting the typical high release probability of this neocortical cell type (Xiang et al., 2002; Bacci et al., 2003a).

Precise spike timing was almost completely recovered in FS cells by artificial but realistic dynamic-clamp autaptic transmission, indicating that autapses play a key role in setting spike timing in FS interneurons and contribute to their highly precise firing. The robust effect of dynamic-clamp-mediated functional autapses in pharmacologically isolated FS interneurons provides direct evidence for a role of GABAergic self-innervation in setting spike timing during sustained firing. This strengthens our conclusion regarding the role of autapses on spike timing based on pharmacological blockade with gabazine alone, which has the previously mentioned non-autaptic effects.

In control conditions, FS cell spike-timing precision tended to improve with increasing firing frequency (Figure S1). This result rules out the possibility that the decrease of precision in gabazine depended on the frequency change associated with $GABA_A$ receptor blockade. In fact, autaptic blockade consistently decreased faithful spike timing despite the tendency of FS cells to improve spike-timing precision at higher frequencies. The dependence of autaptic transmission on spike timing in FS cells was pronounced across a range of firing frequencies, matching the gamma frequency (40–80 Hz). Neither gabazine application nor artificial autaptic conductances affected the high precision obtained at firing frequencies greater than 90–100 Hz (Figure S1). These data indicate that in FS cells autaptic regulation of spike timing is more prominent within the frequency range that these interneurons usually fire during cortical network oscillations (Whittington et al., 1995; Fisahn et al., 1998; Swadlow et al., 1998). It is thus likely that intrinsic mechanisms are responsible for the low spike jitter across trials at higher frequencies.

Interestingly, artificial application of GABAergic autaptic transmission resulted in a marked increase of spike-timing precision and regularity also in pyramidal neurons. This experiment was important to prove that autaptic inhibition self-triggered by action potential firing is in principle important to powerfully modulate neuronal spike timing. However, even if pyramidal neurons are not self-innervated by inhibitory autapses, they do receive GABAergic feedback inhibition from locally projecting interneurons. It has been shown that FS interneurons can fire action potentials less than 2 ms later than spikes generated by presynaptically connected pyramidal neurons (Galarreta and Hestrin, 2001). It is therefore tempting to speculate that this "spike transmission" can generate powerful and well-timed feedback inhibition onto the same pyramidal cells, resulting in modulating their firing pattern and precision. The results of dynamic-clamp autapses on pyramidal neurons shown here might thus be considered as a more general effect of feedback inhibition on neuronal spike timing. Similar to feedback inhibition, it has been shown that soma-targeting feedforward inhibition both in hippocampal pyramidal neurons (Pouille and Scanziani, 2001) and layer IV neocortical RS neurons (Gabernet et al., 2005) is crucial in narrowing the temporal integration window of excitation, precisely locking the timing of a postsynaptic spike to its presynaptic excitation source.

How do GABAergic autapses modulate spike-timing precision? Two possible mechanisms might underlie this phenomenon: after the first AP, the timing of subsequent spikes could be modulated by a change in the membrane time constant due to activation of inter-spike autaptic conductances (conductance effect); alternatively, properly timed hyperpolarizing autaptic events might increase firing probability, possibly through a reduction of sodium channel inactivation (voltage effect; Mainen and Sejnowski, 1995). We have previously shown that autaptic inhibitory responses decrease firing probability from resting membrane potential through the activation of a conductance-mediated electrical shunt (Bacci et al., 2003a). However, during a sustained spike train, the inter-spike membrane potential is relatively depolarized, thus making autaptic transmission hyperpolarizing. We found that dynamic-clamp-generated current-based autaptic hyperpolarizations increase spike-timing precision to a similar extent as autaptic conductances. Moreover, when a constant GABAergic conductance was introduced, FS cell firing became less faithful, even less precise than that elicited by DC stimulations in the presence of gabazine. These data indicate that the autaptic-dependent increase in precision of spike times can be attributed to a voltage rather than a conductance effect. Moreover, they suggest that the presence of a tonic GABAergic conductance can disrupt spike-timing accuracy.

To better isolate the effect of autapses in modulating spike-timing precision in FS interneurons, we pharmacologically eliminated both excitatory and inhibitory synaptic transmission. However, FS interneurons are the target of many synaptic contacts, and they show high-frequency synaptic activity both in vitro and in vivo (Pare et al., 1998; Hasenstaub et al., 2005). Moreover, synaptic noise has been considered to be important in spike-timing modulation in several brain areas (Mainen and Sejnowski, 1995; Carter and Regehr, 2002; Blitz and Regehr, 2003, 2005; Hasenstaub et al., 2005). We introduced realistic synaptic noise in FS interneurons in the form of ongoing spontaneous synaptic activity, and we measured whether autaptic modulation of spike-timing precision was resistant to synaptic noise. We found that precision of spike times was degraded within repetitive trains in the presence of randomized synaptic activity, and the degree of degradation depended on the size and frequency of sPSCs. This effect of synaptic noise contrasts with previously published results showing high precision

of spike times with noisy, but nonrandomized stimuli (Mainen and Sejnowski, 1995; Blitz and Regehr, 2003, 2005). Despite this noise-induced increase in spike variability, GABAergic unitary autaptic transmission robustly improved spike timing in FS interneurons, indicating that these self-inhibitory structures play a crucial role in controlling spike timing even during intense synaptic bombardment.

GABAergic autaptic transmission undergoes prominent short-term depression during sustained firing, thus representing a strong and plastic contribution to FS cell spike-frequency adaptation. In addition, autaptic transmission plays a role in setting spike regularity, as gabazine application increased spike interval variability in the later portion of the train, an effect completely recovered by addition of computer-generated realistic dynamic-clamp autaptic conductances. Interestingly, a recent report indicates that, in the thalamus, time-locked feedforward inhibition is crucial in setting the spike timing of relay neurons, likely by decreasing the capability of thalamic neurons to fire bursts or doublets (Blitz and Regehr, 2005). Similarly, autaptic transmission during a train would then modulate spike-timing precision in two stages: strong autaptic transmission would prevent spike-frequency adaptation in the early phase, and the weaker residual autaptic transmission would lock the steady-state firing to the most predictable firing pattern for any given frequency. Thus, dynamic modulation of the inter-spike intervals by autapses contributes to the nonadapting and highly precise firing typical of FS interneurons.

The switch of firing properties from adapting to nonadapting and even accelerating when autaptic conductance was artificially increased indicates that different amount of self-innervation might be responsible for different degrees of adaptation in FS cells. Variability of the amount of self-innervation from cell to cell might indeed explain the fact that the averaged effect of gabazine on spike-frequency adaptation was less pronounced than in the presence of unvarying artificial autaptic conductances. We have previously shown that ~20% of FS cells show little functional autaptic transmission (Bacci et al., 2003a), yet all FS cells display a relatively nonadapting firing pattern. This suggests the existence of a homeostatic process whereby FS neurons regulate their excitability as required to maintain their output capacity (cf. Bucher et al., 2005).

Notably, our results show that the amount of GABAergic self-innervation should therefore be taken into consideration when spike-frequency adaptation is used to functionally classify different basket cell subtypes (Gupta et al., 2000). Interestingly, among other physiological functions, spike-frequency adaptation is believed to affect cortical network synchrony (Fuhrmann et al., 2002a).

Autapse-dependent high precision of firing of FS interneurons is a unique feature of this GABAergic cell subtype. The precise and thus predictable timing of their action potential activity might represent a means for FS cells to encode information when synchronizing with other FS cells in the generation of oscillations, which entrain cortical networks, due to powerful perisomatic inhibition, during several sensory and cognitive tasks (Buzsaki and Draguhn, 2004).

Experimental Procedures

In Vitro Slice Preparation and Electrophysiology

Sprague Dawley rats aged P16–P21 were anesthetized with pentobarbital (50 mg/kg), decapitated, and the brains were removed and immersed in "cutting" solution (4ºC) containing 234 mM sucrose, 11 mM glucose, 24 mM $NaHCO_3$, 2.5 mM KCl, 1.25 mM NaH_2PO_4, 10 mM $MgSO_4$, and 0.5 mM $CaCl_2$, gassed with 95% O_2 and 5% CO_2. Coronal slices (300 μm) were cut with a vibratome from a block of brain containing sensorimotor cortex. Slices were then incubated in oxygenated artificial cerebrospinal fluid (ACSF) containing 126 mM NaCl, 26 mM $NaHCO_3$, 2.5 mM KCl, 1.25 mM NaH_2PO_4, 2 mM $MgSO_4$, 2 mM $CaCl_2$, and 10 mM glucose; pH 7.4), initially at 32ºC for 1 hr, and subsequently at room temperature, before being transferred to the recording chamber. Recordings were obtained at 32ºC from layer V interneurons visually identified using infrared video microscopy. Firing behavior in current-clamp together with the absence of a large emerging apical dendrite was used to distinguish interneurons from pyramidal neurons. Intracellular labeling with biocytin was used to confirm the interneuronal morphology in some cells (data not shown, but see Bacci et al., 2003a, 2003b). For all current-clamp experiments, whole-cell patch-clamp electrodes (tip resistance = 2–3 MOhm) were filled with an intracellular solution containing 130 mM Kgluconate, 10 mM KCl, 2 mM NaCl, 10 mM HEPES, and 10 mM EGTA; pH = 7.3 corrected with KOH; 290 mOsm. The estimated E_{Cl} was approximately −60 mV based on the Nernst equation, without correction for gluconate-generated liquid junction-potential. For voltage-clamp experiments, the pipette solution contained 70 mM Kgluconate, 70 mM KCl, 2 mM NaCl, 10 mM HEPES, and 10 mM EGTA; pH = 7.3 corrected with KOH; 290 mOsm. The estimated E_{Cl} was approximately −16 mV based on the Nernst equation. Under these recording conditions, activation of $GABA_A$ receptors resulted in easily detectable inward currents at a holding potential (V_h) of −70 mV. Drugs were delivered with a local perfusion system composed of multiple fine tubes ending in a common outlet tube, positioned in proximity (~250 μM) to the recorded neuron. All the experiments were performed including 20 μM 6, 7-dinitroquinoxaline-2,3,dione (DNQX) and 100 μM DL-2-amino-5-posphonovaleric acid (DL-APV) in the bath and local perfusate. Signals were amplified, using a Multiclamp 700A patch-clamp amplifier (Axon Instruments, USA), sampled at 20 KHz, filtered at 10 KHz, and stored on a computer. Data were analyzed using PClamp (Axon Instruments, USA) and Origin (Microcal Inc., USA) software. Locally written software (J.R.H.) was used for spike analysis. FS cells were discarded if they did not show the presence of functional autaptic transmission.

To estimate spike regularity, we used the method described by Holt and collaborators (Holt et al., 1996). Assuming that spikes in a train occur at times t_i ($0 \leq i \leq N$), then the inter-spike interval (ISI) is defined as:

$$\Delta t_i = t_i - t_{i-1}.$$

We calculated the interspike interval CV2 using the following equation:

$$CV2 = (2|\Delta t_{i+1} - \Delta t_i|)/(\Delta t_{i+1} + \Delta t_i).$$

The variability of action potential discharge during a train is better estimated by CV2 rather than the standard method of coefficient of variation ($CV = \sigma_{\Delta t}/<\Delta t>$), as CV2 compares adjacent intervals and is then independent of variations in average firing rates (Holt et al., 1996). Increased CV2 reflects an increased interval-to-interval variability and thus a decreased regularity of spike firing.

Unless otherwise noted, results are presented as means ± SEM. Data were statistically compared using the Student's t test, and differences were considered different if $p < 0.05$.

Autaptic and Synaptic Dynamic clamp

We used a real-time variant of the Linux operating system to implement the dynamic clamp, an approach similar to that used by other groups (Butera et al., 2001; Dorval et al., 2001). We used the Real Time Application Interface RTAI (www.aero.polimi.it/~rtai/), which provides for an event- and/or time-driven analog and digital interface with a biological system. This real-time system was coupled

with the open source COMEDI project (www.comedi.org), which provides a set of drivers for data acquisition boards, and the power of open source compilers (e.g., gcc), and allows for rapid development of dynamic-clamp applications. We ran the dynamic clamp on a separate computer from our experimental data acquisition computer so that dynamic-clamp output (i.e., individual conductances and currents) could be recorded and verified. To maintain accurate dynamic clamp, bridge balance was monitored and compensated periodically throughout the experiment. The autaptic conductance was triggered by actual spikes evoked either in FS interneurons or pyramidal cells. The biophysical properties of the autaptic conductance were derived after analyzing single autaptic responses obtained from >80 FS interneurons, and they were similar to those already reported (Bacci et al., 2003a). Single dynamic-clamp autapses had a peak conductance of 6 nS, a decay time constant of 6.8 ms, a chloride reversal potential of −65 mV with a delay of 1 ms following each spike. Total autaptic conductance was incremented after each spike according to resource availability (see below). During spike trains, dynamic-clamp autapses depressed, following the decrease of available neurotransmitter resources, based on the equation derived by Fuhrmann and collaborators (Fuhrmann et al., 2002b):

$$dR/dt = (1 - R)/\tau_{rec} - U_{SE} \times R \times \delta(t - t_{sp}),$$

where R is the neurotransmitter resource, i.e., the available neurotransmitter at the presynaptic terminal, U_{SE} is the fraction of the available neurotransmitter pool to be utilized, τ_{rec} is the autaptic depression recovery time constant, and t_{sp} the time at which a presynaptic action potential occurs. The values of U_{SE} (30%) and τ_{rec} (100 ms) were estimated based on the experiments in Figure 2 and were assumed to be time and voltage independent. Current-based IPSCs were calculated using a fixed driving force of 10 mV.

Synaptic dynamic clamp was generated according to sIPSC and sEPSC properties recorded in FS interneurons in cortical slices (see below, Figure S3, and Bacci et al., 2003b). sPSCs with random normally distributed amplitudes were generated according to a Poisson process, and amplitudes and times were re-shuffled before each sweep. Each stimulation protocol consisted of ten sweeps containing stochastically different synaptic activity. We generated four protocols: with sPSC low frequency and amplitude, with sPSC high amplitude and low frequency, with sPSC high frequency and low amplitude, and with sPSC high frequency and amplitude. Although sPSCs were re-shuffled before each sweep within a protocol series, identical stimulus protocol series were repeated in the presence and in the absence of autaptic conductance. Dynamic-clamp-generated sPSCs started 150 ms before and ended 200 ms after 600 ms long DC steps used to initiate repetitive firing. sEPSCs had a decay time constant (τ) of 1.58 ms, a reversal potential of 0 mV, a peak conductance of 0.25 ± 0.25 nS (mean ± SD) for the low-amplitude protocols, and 0.75 ± 0.75 nS for the high-amplitude protocols. sEPSC frequency was 20 and 200 Hz for the low- and high-frequency protocols, respectively. sIPSCs had a decay time constant (τ) of 6.8 ms, a reversal potential of −65 mV, an averaged conductance of 0.5 ± 0.4 nS for the low-amplitude protocols, and 1.5 ± 1.2 nS for the high-amplitude protocols. sIPSC frequency was 5 and 50 Hz for the low- and high-frequency protocols, respectively.

Supplemental Data

The Supplemental Data for this article can be found online at http://www.neuron.org/cgi/content/full/49/1/119/DC1/.

Acknowledgments

We would like to thank Vikaas S. Sohal for assistance with preliminary versions of the Linux/RTAI-based dynamic clamp. This work was supported by NIH grants NS39579 from the NINDS.

Received: August 9, 2005
Revised: November 22, 2005
Accepted: December 15, 2005
Published: January 4, 2006

References

Bacci, A., Huguenard, J.R., and Prince, D.A. (2003a). Functional autaptic neurotransmission in fast-spiking interneurons: a novel form of feedback inhibition in the neocortex. J. Neurosci. *23*, 859–866.

Bacci, A., Rudolph, U., Huguenard, J.R., and Prince, D.A. (2003b). Major differences in inhibitory synaptic transmission onto two neocortical interneuron subclasses. J. Neurosci. *23*, 9664–9674.

Beierlein, M., Gibson, J.R., and Connors, B.W. (2000). A network of electrically coupled interneurons drives synchronized inhibition in neocortex. Nat. Neurosci. *3*, 904–910.

Beierlein, M., Gibson, J.R., and Connors, B.W. (2003). Two dynamically distinct inhibitory networks in layer 4 of the neocortex. J. Neurophysiol. *90*, 2987–3000.

Blitz, D.M., and Regehr, W.G. (2003). Retinogeniculate synaptic properties controlling spike number and timing in relay neurons. J. Neurophysiol. *90*, 2438–2450.

Blitz, D.M., and Regehr, W.G. (2005). Timing and specificity of feed-forward inhibition within the LGN. Neuron *45*, 917–928.

Bucher, D., Prinz, A.A., and Marder, E. (2005). Animal-to-animal variability in motor pattern production in adults and during growth. J. Neurosci. *25*, 1611–1619.

Buracas, G.T., Zador, A.M., DeWeese, M.R., and Albright, T.D. (1998). Efficient discrimination of temporal patterns by motion-sensitive neurons in primate visual cortex. Neuron *20*, 959–969.

Butera, R.J., Jr., Wilson, C.G., Delnegro, C.A., and Smith, J.C. (2001). A methodology for achieving high-speed rates for artificial conductance injection in electrically excitable biological cells. IEEE Trans. Biomed. Eng. *48*, 1460–1470.

Buzsaki, G., and Draguhn, A. (2004). Neuronal oscillations in cortical networks. Science *304*, 1926–1929.

Carandini, M. (2004). Amplification of trial-to-trial response variability by neurons in visual cortex. PLoS Biol. *2*, E264.

Carter, A.G., and Regehr, W.G. (2002). Quantal events shape cerebellar interneuron firing. Nat. Neurosci. *5*, 1309–1318.

de Ruyter Van Steveninck, R.R., Lewen, G.D., Strong, S.P., Koberle, R., and Bialek, W. (1997). Reproducibility and variability in neural spike trains. Science *275*, 1805–1808.

Dorval, A.D., Christini, D.J., and White, J.A. (2001). Real-time linux dynamic clamp: a fast and flexible way to construct virtual ion channels in living cells. Ann. Biomed. Eng. *29*, 897–907.

Fairhall, A.L., Lewen, G.D., Bialek, W., and de Ruyter Van Steveninck, R.R. (2001). Efficiency and ambiguity in an adaptive neural code. Nature *412*, 787–792.

Farrant, M., and Nusser, Z. (2005). Variations on an inhibitory theme: phasic and tonic activation of GABA(A) receptors. Nat. Rev. Neurosci. *6*, 215–229.

Fisahn, A., Pike, F.G., Buhl, E.H., and Paulsen, O. (1998). Cholinergic induction of network oscillations at 40 Hz in the hippocampus in vitro. Nature *394*, 186–189.

Freund, T.F. (2003). Interneuron diversity series: Rhythm and mood in perisomatic inhibition. Trends Neurosci. *26*, 489–495.

Fricker, D., and Miles, R. (2001). Interneurons, spike timing, and perception. Neuron *32*, 771–774.

Fuhrmann, G., Markram, H., and Tsodyks, M. (2002a). Spike frequency adaptation and neocortical rhythms. J. Neurophysiol. *88*, 761–770.

Fuhrmann, G., Segev, I., Markram, H., and Tsodyks, M. (2002b). Coding of temporal information by activity-dependent synapses. J. Neurophysiol. *87*, 140–148.

Gabernet, L., Jadhav, S.P., Feldman, D.E., Carandini, M., and Scanziani, M. (2005). Somatosensory integration controlled by dynamic thalamocortical feed-forward inhibition. Neuron *48*, 315–327.

Galarreta, M., and Hestrin, S. (1999). A network of fast-spiking cells in the neocortex connected by electrical synapses. Nature *402*, 72–75.

Galarreta, M., and Hestrin, S. (2001). Spike transmission and synchrony detection in networks of GABAergic interneurons. Science *292*, 2295–2299.

Gibson, J.R., Beierlein, M., and Connors, B.W. (1999). Two networks of electrically coupled inhibitory neurons in neocortex. Nature *402*, 75–79.

Grothe, B., and Klump, G.M. (2000). Temporal processing in sensory systems. Curr. Opin. Neurobiol. *10*, 467–473.

Gupta, A., Wang, Y., and Markram, H. (2000). Organizing principles for a diversity of GABAergic interneurons and synapses in the neocortex. Science *287*, 273–278.

Gur, M., Beylin, A., and Snodderly, D.M. (1997). Response variability of neurons in primary visual cortex (V1) of alert monkeys. J. Neurosci. *17*, 2914–2920.

Hajos, N., Palhalmi, J., Mann, E.O., Nemeth, B., Paulsen, O., and Freund, T.F. (2004). Spike timing of distinct types of GABAergic interneuron during hippocampal gamma oscillations in vitro. J. Neurosci. *24*, 9127–9137.

Hasenstaub, A., Shu, Y., Haider, B., Kraushaar, U., Duque, A., and McCormick, D.A. (2005). Inhibitory postsynaptic potentials carry synchronized frequency information in active cortical networks. Neuron *47*, 423–435.

Holt, G.R., Softky, W.R., Koch, C., and Douglas, R.J. (1996). Comparison of discharge variability in vitro and in vivo in cat visual cortex neurons. J. Neurophysiol. *75*, 1806–1814.

Huguenard, J.R., and Alger, B.E. (1986). Whole-cell voltage-clamp study of the fading of GABA-activated currents in acutely dissociated hippocampal neurons. J. Neurophysiol. *56*, 1–18.

Kara, P., Reinagel, P., and Reid, R.C. (2000). Low response variability in simultaneously recorded retinal, thalamic, and cortical neurons. Neuron *27*, 635–646.

Kawaguchi, Y., and Kubota, Y. (1997). GABAergic cell subtypes and their synaptic connections in rat frontal cortex. Cereb. Cortex *7*, 476–486.

Kawaguchi, Y., and Kubota, Y. (1998). Neurochemical features and synaptic connections of large physiologically-identified GABAergic cells in the rat frontal cortex. Neuroscience *85*, 677–701.

Klausberger, T., Magill, P.J., Marton, L.F., Roberts, J.D., Cobden, P.M., Buzsaki, G., and Somogyi, P. (2003). Brain-state- and cell-type-specific firing of hippocampal interneurons in vivo. Nature *421*, 844–848.

Mainen, Z.F., and Sejnowski, T.J. (1995). Reliability of spike timing in neocortical neurons. Science *268*, 1503–1506.

McBain, C.J., and Fisahn, A. (2001). Interneurons unbound. Nat. Rev. Neurosci. *2*, 11–23.

Pare, D., Shink, E., Gaudreau, H., Destexhe, A., and Lang, E.J. (1998). Impact of spontaneous synaptic activity on the resting properties of cat neocortical pyramidal neurons In vivo. J. Neurophysiol. *79*, 1450–1460.

Penttonen, M., Kamondi, A., Acsady, L., and Buzsaki, G. (1998). Gamma frequency oscillation in the hippocampus of the rat: intracellular analysis in vivo. Eur. J. Neurosci. *10*, 718–728.

Pouille, F., and Scanziani, M. (2001). Enforcement of temporal fidelity in pyramidal cells by somatic feed-forward inhibition. Science *293*, 1159–1163.

Reich, D.S., Victor, J.D., Knight, B.W., Ozaki, T., and Kaplan, E. (1997). Response variability and timing precision of neuronal spike trains in vivo. J. Neurophysiol. *77*, 2836–2841.

Reinagel, P., and Reid, R.C. (2002). Precise firing events are conserved across neurons. J. Neurosci. *22*, 6837–6841.

Schreiber, S., Fellous, J.M., Tiesinga, P., and Sejnowski, T.J. (2004). Influence of ionic conductances on spike timing reliability of cortical neurons for suprathreshold rhythmic inputs. J. Neurophysiol. *91*, 194–205.

Semyanov, A., Walker, M.C., Kullmann, D.M., and Silver, R.A. (2004). Tonically active GABA A receptors: modulating gain and maintaining the tone. Trends Neurosci. *27*, 262–269.

Shadlen, M.N., and Newsome, W.T. (1998). The variable discharge of cortical neurons: implications for connectivity, computation, and information coding. J. Neurosci. *18*, 3870–3896.

Somogyi, P., and Klausberger, T. (2005). Defined types of cortical interneurone structure space and spike timing in the hippocampus. J. Physiol. *562*, 9–26.

Stell, B.M., and Mody, I. (2002). Receptors with different affinities mediate phasic and tonic GABA(A) conductances in hippocampal neurons. J. Neurosci. *22*, RC223.

Stevens, C.F., and Zador, A. (1995). Neural coding: The enigma of the brain. Curr. Biol. *5*, 1370–1371.

Swadlow, H.A., Beloozerova, I.N., and Sirota, M.G. (1998). Sharp, local synchrony among putative feed-forward inhibitory interneurons of rabbit somatosensory cortex. J. Neurophysiol. *79*, 567–582.

Tamas, G., Buhl, E.H., and Somogyi, P. (1997a). Fast IPSPs elicited via multiple synaptic release sites by different types of GABAergic neurone in the cat visual cortex. J. Physiol. *500*, 715–738.

Tamas, G., Buhl, E.H., and Somogyi, P. (1997b). Massive autaptic self-innervation of GABAergic neurons in cat visual cortex. J. Neurosci. *17*, 6352–6364.

Tamas, G., Somogyi, P., and Buhl, E.H. (1998). Differentially interconnected networks of GABAergic interneurons in the visual cortex of the cat. J. Neurosci. *18*, 4255–4270.

Tamas, G., Buhl, E.H., Lorincz, A., and Somogyi, P. (2000). Proximally targeted GABAergic synapses and gap junctions synchronize cortical interneurons. Nat. Neurosci. *3*, 366–371.

Thomson, A.M., West, D.C., Hahn, J., and Deuchars, J. (1996). Single axon IPSPs elicited in pyramidal cells by three classes of interneurones in slices of rat neocortex. J. Physiol. *496*, 81–102.

VanRullen, R., Guyonneau, R., and Thorpe, S.J. (2005). Spike times make sense. Trends Neurosci. *28*, 1–4.

Whittington, M.A., Traub, R.D., and Jefferys, J.G. (1995). Synchronized oscillations in interneuron networks driven by metabotropic glutamate receptor activation. Nature *373*, 612–615.

Xiang, Z., Huguenard, J.R., and Prince, D.A. (2002). Synaptic inhibition of pyramidal cells evoked by different interneuronal subtypes in layer v of rat visual cortex. J. Neurophysiol. *88*, 740–750.